NEW SIMPLE MODELS FOR FAST ADSORPTION AND/OR DIFFUSION CALCULATIONS IN A SINGLE SPHERICAL PARTICLE

René Alejandro Mora-Casal[1]*, José Rafael Mora-Casal[2]

[1]*Escuela de Ingeniería Química, Ciudad de la Investigación, Universidad de Costa Rica, Costa Rica*
[2]*Consultor privado, Tibás, Costa Rica*

Abstract

Five approximate models were developed for the mean intraparticle concentration during adsorption and/or diffusion with negligible external resistance ($Bi \rightarrow \infty$); all of them are more accurate that the reference model of Do and Mayfield (1987). Their simplicity makes them applicable for the design of batch and fixed-bed adsorbers. Three of the models are based on a n-order profile for the intraparticle concentration with a time-dependent exponent n. Other two new models were obtained by analysis and algebraic manipulation of the $\overline{A}(\tau)$ data. Graphical visualization and numerical optimization were used to develop the models and to assess their quality. The selection of a particular model will depend of the required accuracy. The approach described in this work can be applied to more complex models, such as non-linear isotherms, multicomponent adsorption and branched pore structure.

Resumen

Se elaboraron cinco modelos aproximados para la concentración intrapartícula promedio durante la adsorción y/o difusión con resistencia externa despreciable ($Bi \rightarrow \infty$); todos ellos son más exactos que el modelo de referencia de Do & Mayfield (1987). Su simplicidad los hace aplicables para el diseño de adsorbedores por lotes y de lecho fijo. Tres de los modelos se basan en un perfil de orden n para la concentración intrapartícula con un exponente n dependiente del tiempo. Se obtuvieron otros dos nuevos modelos mediante el análisis y manipulación algebraica de los datos $\overline{A}(\tau)$. Se utilizó la visualización gráfica y la optimización numérica para desarrollar los modelos y evaluar su calidad. La selección de un modelo particular dependerá de la precisión requerida. El enfoque descrito en este trabajo se puede aplicar a modelos más complejos, tales como isotermas no lineales, la adsorción multicomponente y estructuras de poro ramificado.

I. INTRODUCTION

In order to study and design adsorption systems, the concentration inside the adsorbent particles must be predicted and a model must be assumed. The exact model is an infinite series that is slowly convergent and computationally intensive; for that reason, approximate models have been proposed to reproduce the intraparticle concentration profile within a predefined error margin. The approximate model mostly used is the Linear Driving Force (LDF) one, first formulated and recommended by Glueckauf (1955):

$$\frac{\partial \overline{q}}{\partial t} = \frac{15D_e}{R^2}(q - \overline{q}) \tag{1}$$

Due to its simplicity, the LDF model has been used by many authors (Garg & Ruthven, 1975; Kim, 1989; Do & Rice, 1990; Sircar & Hufton, 2000 and 2000a; Subramanian et al, 2001; Kim, 2009). A problem this model has is that of predicting negative adsorption at certain values, as shown by Do &

---

* Corresponding author: *rene.moracasal@ucr.ac.cr*

Mayfield (1987) and Li & Yang (1999). These authors proposed a generalized concentration profile to overcome these unrealistic results, as follows:

$$A(x, \tau) = a_0(\tau) + a_1(\tau) \cdot x^n \tag{2}$$

Li & Yang (1999) and Sircar & Hufton (2000) proposed integer n values. Do & Mayfield (1987) proposed n to be a continuous function of time, showing several ways to define this function. They obtained an improvement with one of their models, when compared to the parabolic profile one; however, their relative error is still 19% at x = 0.001 (an 86% for the later model).

The purpose of this work is to make a critical review of the Do & Mayfield results, in order to propose three new functional forms for n which represent an improvement in the calculation of the mean internal concentration. Other two new models are proposed by analysis and algebraic manipulation of the $A(\tau)$ data. Graphical visualization and numerical optimization will be used to develop the models and to assess their quality.

II. THEORY AND FORMER MODELS

The non-dimensional equation and boundary conditions for the intraparticle adsorption are:

$$\frac{\partial A}{\partial \tau} = \frac{1}{x^2} \frac{\partial}{\partial x}\left(x^2 \frac{\partial A}{\partial x}\right) \tag{3}$$

$\tau = 0; A = 0$
$x = 0; \ \partial A/\partial x = 0$
$x = 1; \ \partial A/\partial x = Bi(1 - A)$

A is the non-dimensional intraparticle concentration profile (C/C_0 or q/KC_0), x and τ are the non-dimensional length and time respectively, and Bi is the Biot number ($k_m R/D_e$ or $k_m R/\rho_P K D_s$) containing the mass transfer coefficient k_m. Different definitions apply depending on whether the pore diffusion or the solid diffusion model is considered (Weber & Chakravorty, 1974; Do & Rice, 1986; Do & Mayfield, 1987). The interest for the present work lays in the solution when the external mass transfer resistance is negligible (Bi or k_m infinite), it can be obtained by separation of variables (Li & Yang, 1999; Sircar & Hufton, 2000), where $\overline{A}$ is the mean intraparticle solute concentration, as well as a measure of the fractional uptake (Do & Mayfield, 1987):

$$\overline{A} = 1 - 6 \sum_{k=1}^{\infty} \frac{e^{-(\pi k)^2 \tau}}{(\pi k)^2} \tag{4}$$

This formula is slowly convergent and requires 100 terms to reach a six-decimal place accuracy at low values of τ, as shown in Table 1. The LDF approximation assumes that the mean intraparticle concentration can be obtained from the following equation, which is equivalent to the one proposed by Glueckauf and whose solution is an exponential (Do & Mayfield, 1987):

$$\frac{\partial \overline{A}}{\partial \tau} = \frac{15(1 - \overline{A})}{(1 + 5/Bi)} \tag{5}$$

Liaw (1979) showed that this equation can be obtained if a parabolic intraparticle concentration profile is assumed. Li & Yang (1999) demonstrated that the LDF formula can be obtained from a general n-power particle profile, represented by Equation (2) where n is an integer. The parabolic profile would be a special case of this model when n = 2.

Table 1. Exact values of the intraparticle concentration and number of terms in the infinite series required to calculate them.

τ	$\overline{A}$	# of terms
0.0001	0.033551	100
0.001	0.104047	100
0.01	0.308514	84
0.02	0.418731	59
0.05	0.606940	37
0.1	0.770479	26
0.2	0.915496	18
0.5	0.995628	11
1	0.999969	8
2	1.000000	5
5	1.000000	3
10	1.000000	2
20	1.000000	1

A problem of the LDF model is that of predicting negative adsorption at certain values with the parabolic profile, according to Do & Mayfield (1987) and Li & Yang (1999). The later authors recommended n = 5 instead of n = 2 in order to avoid this situation. This result was challenged by Sircar & Hufton (2000a), who demonstrated that n can take any positive integer value n ≥ 2 and found an error in one of the equations of Li & Yang. Sircar & Hufton also showed that a general intraparticle profile is compatible with the LDF model:

$$A(x,\tau) = a(\tau) + b(\tau) * F(x) \tag{6}$$

A different approach was taken by Do & Mayfield (1987), who proposed n to be a continuous and decreasing function of time. The following results were obtained:

$$n = 0.123\tau^{-0.68} \tag{7}$$

$$\frac{\partial \overline{A}}{\partial \tau} = \frac{3(n+3)}{\left[1 + \frac{(n+3)}{Bi}\right]}(1 - \overline{A}) \tag{8}$$

$$\overline{A} = 1 - \exp[-9\tau - 1.153\tau^{0.32}] \text{ for } Bi \to \infty \tag{9}$$

Equation (12) in Do & Mayfield article has the wrong exponent (0.638 instead of 0.68). Note also that a value of 15 in the coefficient of Equation (8) is obtained if n = 2 only. Inspecting Figure 2 in Do & Mayfield (1987), the expression for n is valid in the interval $\tau = (0.002, 0.2)$ only and the points follow a curve instead of a straight line. Thus there is room for improvement if a larger interval is taken or if the values of n are adjusted to a curve instead of a straight line.

Another approach, not considered before, can be developed if the $\overline{A}(\tau)$ curve is plotted on a log-log scale, as in Figure 1 below. Notice that the curve follows a square-root law for small values of τ (we included a line representing it for comparison), while $\overline{A}$ takes a constant value of unity for larger values of τ. This information will be used to develop a new approximation for $\overline{A}(\tau)$.
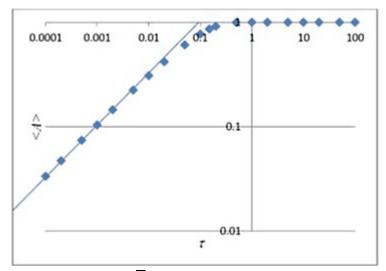
Figure 1. Plot of $\overline{A}$ as a function of τ on a log-log scale.

III. DEVELOPMENT OF THE MODELS

Model #1:

Do & Mayfield (1987) defined an auxiliary variable n^*, related to the exponent of the intraparticle profile n as follows:

$$n^* = \frac{1}{\tau}\int_0^{\tau} n \, d\tau = 0.385\tau^{-0.68} \tag{10}$$

The constants were obtained by data regression in the interval $\tau = (0.002, 0.2)$ as it is shown by the red line in Figure 2. The adjustment seems adequate for the selected interval, but it deviates from the data for smaller values of n^*. $\overline{A}$ values show a deviation of +22% at x = 0.001 and of +77% at x = 0.0001. The n^* values at smaller times are more critical because they represent the initial stages of adsorption and the $\overline{A}$ values are very small. For x ≥ 0.2, $\overline{A}$ values are almost unity and they become insensitive to the values of n or n^*.
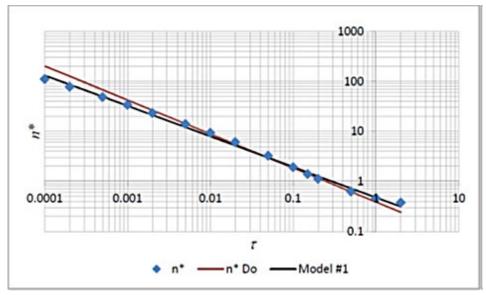

Figure 2. Plot of n^* as a function of τ, showing adjustment by
Do & Mayfield (1987) and Model #1.

Taking a larger interval allows one to obtain a better agreement between model and data. Considering interval (0.0001, 0.5), the results of the adjustment to a potential model are as follows:

$$n^* = 0.4728\tau^{-0.6117} \tag{11}$$

$$n = 0.1836\tau^{-0.6117} \tag{12}$$

$$\overline{A} = 1 - \exp[-9\tau - 1.4184\tau^{0.3883}] \text{ for } Bi \to \infty \tag{13}$$

There is a significant improvement with the new model: the $\overline{A}$ values show a deviation of -3.3% at x = 0.001 and of $+19\%$ at x = 0.0001. This model is represented by the black line in Figure 2 for n^* values, and the $\overline{A}$ curve is plotted in Figure 4 below.

Model #2:

A closer examination of Figure 2 allows one to conclude that the n^* values follow a curve instead of a straight line in the interval (0.0001, 0.5). The point of inflexion around x = 0.5 will be ignored in order to obtain a simpler model, also because the $\overline{A}$ values become insensitive to the n values for x > 0.2, as explained for the Model #1. The n^* values can be adjusted to the following expression for the selected interval; this is shown as the red curve in Figure 3:

$$\ln n^* = -1.06694 - 0.79410 \ln \tau - 0.018433(\ln \tau)^2$$

$$n^* = 0.3441\tau^{-0.79410-0.018433\ln\tau} \tag{14}$$
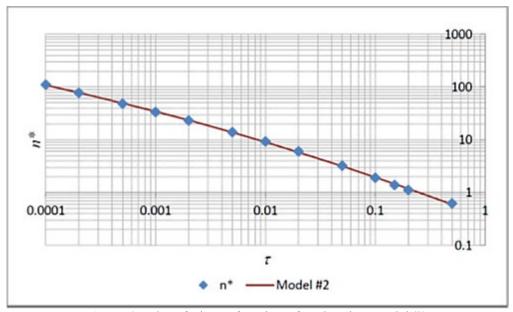

Figure 3. Plot of n* as a function of τ, showing Model #2.

The $\overline{A}$ values can be calculated with an expression obtained by Do & Mayfield (1987):

$$\overline{A} = 1 - \exp[-3(n^* + 3)\tau] \text{ for } Bi \to \infty \tag{15}$$

$$\overline{A} = 1 - \exp\left[-9\tau - 1.0322\tau^{0.2059-0.018433\ln\tau}\right] \tag{16}$$

There is an additional improvement with this model, compared with Model #1: the $\overline{A}$ values show a deviation of $+2.1\%$ at x = 0.001 and of -2.3% at x = 0.0001. The following figure compares the Do & Mayfield model and Models #1 and #2 with the exact values, on a ratio basis:
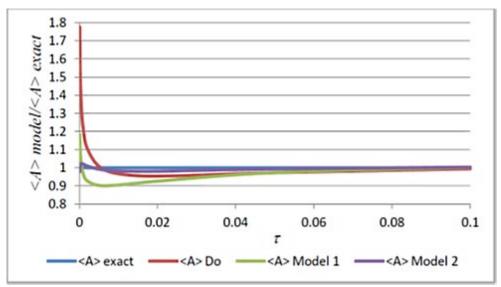
Figure 4. Comparison of the discussed models, on a ratio basis.

Models #3 and #4:

It was shown in Figure 1 above that $\overline{A}(\tau)$ has asymptotic behavior, going towards a function $C\sqrt{\tau}$ when $\tau \to 0$ and approaching unity for $\tau \geq 1$. By algebraic modifications, a function $G(\tau)$ with exponential decay is obtained, as illustrated in Table 2 and Figure 5.

Table 2. Modifications of function $\overline{A}(\tau)$ and their asymptotic behavior

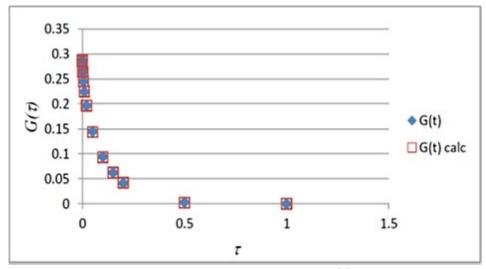| Function	$\tau \to 0$	$\tau \to \infty$
$\overline{A}(\tau)$	$C\sqrt{\tau}$	1
$\overline{A}(\tau)/\sqrt{\tau}$	C	$1/\sqrt{\tau}$
$\sqrt{\tau}/\overline{A}(\tau)$	$1/C$	$\sqrt{\tau}$
$G(\tau) = \dfrac{\sqrt{\tau}}{\overline{A}(\tau)} - \sqrt{\tau}$	$1/C'$	0

Figure 5. Behavior of function $G(\tau)$.

Further examination of the function $G(\tau)$ shows that it has the form $P(\sqrt{\tau})e^{-k\tau}$; thus the following expression is postulated:

$$G(\tau) = \left(A + B\sqrt{\tau} + C\tau\right)\left(D + Ee^{-k\tau}\right) \tag{17}$$

The constants were found by use of an optimization program (Solver option in MS Excel), and it was determined that $D = 0$. The final form of the function is:

$$G(\tau) = \left(0.29410 - 0.67553\sqrt{\tau} + 0.38392\tau\right)e^{-2.4214\tau} \tag{18}$$

This function is represented by the red squares in Figure 5 above. Model #3 was obtained by going from $G(\tau)$ to $\overline{A}(\tau)$ by algebraic manipulations:

$$G(\tau) = \left(A - B\sqrt{\tau} + C\tau\right)e^{-k\tau}$$
$$\frac{\sqrt{\tau}}{\overline{A}(\tau)} - \sqrt{\tau} = \left(A - B\sqrt{\tau} + C\tau\right)e^{-k\tau}$$
$$\frac{1}{\overline{A}(\tau)} = 1 + \frac{\left(A - B\sqrt{\tau} + C\tau\right)e^{-k\tau}}{\sqrt{\tau}} \tag{19}$$
$$\overline{A}(\tau) = \frac{\sqrt{\tau}}{\sqrt{\tau} + \left(A - B\sqrt{\tau} + C\tau\right)e^{-k\tau}}$$

In the above equations, constant E was absorbed into the other constants, and the negative sign of B was incorporated into the formula. This model was adjusted against the exact model of $\overline{A}(\tau)$ (using the Solver option) and the values of the constants changed slightly as follows:

$$\overline{A}(\tau) = \frac{\sqrt{\tau}}{\sqrt{\tau} + \left(0.29072 - 0.61963\sqrt{\tau} + 0.31866\tau\right)e^{-3.0390\tau}} \tag{20}$$

Model #3 shows a remarkable agreement against the exact values, showing a deviation of +0.6% at x = 0.001 and of +1.2% at x = 0.0001.

Although Model #3 does not have negative values in the interval (0.0001, 100), it would be desirable to have positive coefficients only in the model. Based on the approximation $(1 - x)^{-1} \approx 1 + x$, another model is generated by assuming a positive sign before B and putting the quadratic polynomial in the denominator of $G(\tau)$, as follows:

$$G(\tau) = \frac{Ee^{-k\tau}}{\left(A + B\sqrt{\tau} + C\tau\right)}$$
$$\frac{\sqrt{\tau}}{\overline{A}(\tau)} - \sqrt{\tau} = \frac{Ee^{-k\tau}}{\left(A + B\sqrt{\tau} + C\tau\right)}$$
$$\frac{1}{\overline{A}(\tau)} = 1 + \frac{Ee^{-k\tau}}{\left(A + B\sqrt{\tau} + C\tau\right)\sqrt{\tau}}$$
$$\overline{A}(\tau) = \frac{\left(A + B\sqrt{\tau} + C\tau\right)\sqrt{\tau}}{\left(A + B\sqrt{\tau} + C\tau\right)\sqrt{\tau} + Ee^{-k\tau}} \tag{21}$$

This Model #4 was adjusted against the exact model of $\overline{A}$ (using the Solver option) and there were some changes in the values of the constants as follows:

$$\overline{A}(\tau) = \frac{\left(0.29410 + 0.64595\sqrt{\tau} - 0.61278\tau\right)\sqrt{\tau}}{\left(0.29410 + 0.64595\sqrt{\tau} - 0.61278\tau\right)\sqrt{\tau} + 0.085439e^{-7.4056\tau}} \tag{22}$$

Notice that coefficient k shows the greatest variation (from –3.039 to –7.406), and that a negative coefficient was unavoidable, in this case constant C. Model #4 also shows a remarkable agreement against exact values, with a deviation of +0.7% at x = 0.001 and of +1.3% at x = 0.0001. Figure 6 below compares the four models developed here with the exact values on a ratio basis:
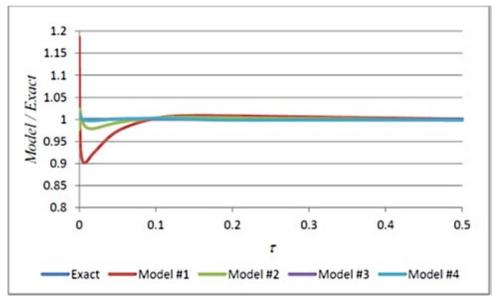

Figure 6. Comparison of the four models on a ratio basis.

IV.   DISCUSSION

Many years ago, before the construction and use of the first electronic computers, researchers had to be very creative analyzing data and extracting useful information to develop correlations or test theoretical models. They relayed on graphical methods to visualize trends and find the constants of their models: these visualization techniques remain valid and relevant today, since they can be used to better understand the behavior of process variables, as well as to discriminate between different models or explanations for this behavior. The power of computers and numerical methods included in electronic software (such as MathCAD or the Solver option in MS Excel) allows the researcher to optimize his/her models, so the existing models can be improved and new ones can be developed. Considering that some of the models used in Chemical Engineering today are fifty years old or older, it is possible to affirm that every existing model can be improved: an example is the intensive work in the field of equations of state.

By looking at the Figure 6 above, one could conclude that Models #3 and #4, Equations (20) and (22), are the best ones to approximate the infinite series, but this statement can be refined in further analysis. At the current times of complex models with hundreds of constants, some of the characteristics of a good model –from the own point of view– consist of having a simple formula, a few number of constants, some physical sense or insight and to be easily programmable on a calculator or an electronic worksheet. In that case Model #1, represented by Equation (13), would be the best one because of having four constants, two of them being easy to remember (1 and 9), and by having a simple expression that hints to the physical behavior. These are also the characteristics of the Do & Mayfield model which motivated the present study.

Model #2, represented by Equation (16), introduces one more constant and a higher level of complexity (a logarithm in the exponent), but it is still manageable and maintains physical sense. Model #3 would represent the best model overall since it is better than the two previous ones, due to its five constants; this is the same number as Model #2, but with a simpler formula ($\sqrt{\tau}$ simpler than $\ln \tau$). It is not difficult to enter this model into a worksheet and it has physical insight of a different type (a quotient going to 1, instead of a difference going to 1 in the former models). Model #4 does not represent an improvement over Model #3 because it has one more constant, a more complex formula and, as it will be further discussed, Model #3 follows more closely the exact function.

Notice that the ratio between the approximate and the exact models has an oscillating nature, which also decreases with time. If the agreement between model and data were total their ratio would be always

unity but, with approximate models, the ratio is above unity at some intervals and below unity at others. Table 3 below compares the different models based on this ratio R.

The number of oscillations increases with the complexity of the model: the reference model and Model #1 have only one valley, while Models #3 and 4 have two valleys and one peak. The changing oscillation could be modeled, but this would add unnecessary complexity to the approximate model for practical purposes. By looking at Table 3 below, one can notice that Model #3 is better than Model #4 because the later raises more slowly from the valley at x = 0.5, so the ratio with the exact value reaches unity until x = 2, while Model #3 reaches that value at x = 0.5. The described behaviour can be seen graphically in Figure 7 below.

Table 3. Comparison of the discussed models (ratio basis).

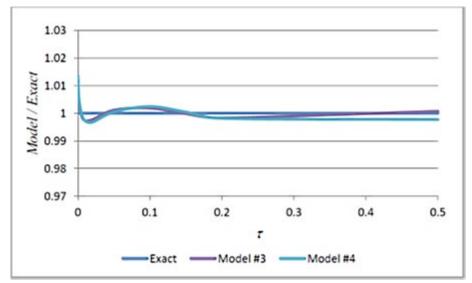| Model	Behavior (peaks and valleys)
Reference model (Do & Mayfield, 1987)	Ratio $R = 1.77$ at $x = 0.0001$. $R = 0.95$ at $x = 0.02$. $R = 1$ for $x \geq 0.5$. Error: +77% to –5%.
Model #1	Ratio $R = 1.19$ at $x = 0.0001$. $R = 0.90$ at $x = 0.005$. $R = 1$ for $x \geq 0.5$. Error: +19% to –10%.
Model #2	Ratio $R = 0.977$ at $x = 0.0001$. $R = 1.023$ at $x = 0.0005$. $R = 0.98$ at $x = 0.02$. $R = 1$ for $x \geq 0.5$. Error: +2.3% to –2.3%.
Model #3	Ratio $R = 1.012$ at $x = 0.0001$. $R = 0.997$ at $x = 0.01$. $R = 1.002$ at $x = 0.1$. $R = 0.998$ at $x = 0.2$. $R = 1$ for $x \geq 0.5$. Error: +1.2% to –0.3%.
Model #4	Ratio $R = 1.013$ at $x = 0.0001$. $R = 0.997$ at $x = 0.02$. $R = 1.002$ at $x = 0.1$. $R = 0.998$ at $x = 0.5$. $R = 1$ for $x \geq 2$. Error: +1.3% to –0.3%.

Figure 7. Comparison between Model #3 and Model #4 (ratio basis).

Regarding Models #1 and #2, their expressions for n^* can be seen as representative of the following class of functions:

$$n^* = K\tau^{a+bf(\tau)} \tag{23}$$

Equation (11) is obtained if $f(\tau) = 0$, and Equation (14) is obtained if $f(\tau) = \ln\tau$. A simpler model can be obtained if the choice $f(\tau) = \tau$ is made, it can be called Model #2B:

$$n^* = K\tau^{a+b\tau} \tag{24}$$

$$n^* = 0.996078\tau^{-0.511855+2.45184\tau} \tag{25}$$

$$\overline{A} = 1 - \exp[-9\tau - 2.988234\tau^{0.488145+2.45184\tau}] \tag{26}$$

Model #2B has a similar form than Model #2, with one valley and one peak. Its values tend to be greater than the exact values, but the error is always less than 2% and the error range is better than Model #2 (it is +1.8% to –0.4%, compared to +2.3% to –2.3% for Model #2). The behavior of Model #2B can be seen in the following figure, where it is compared with both Model #2 and Model #3, the best model found in the present work.
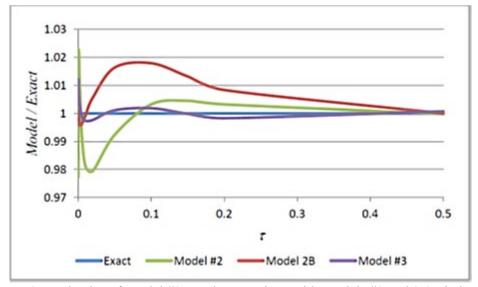

Figure 8 – Behavior of Model #2B and comparison with Models #2 and 3 (ratio basis).

There was still another expression for n proposed by Do & Mayfield (1987), with the form:

$$n = n_0 \frac{1 - \overline{A}}{\overline{A}} \tag{27}$$

If we plot n against $(1 - \overline{A})/\overline{A}$, a curve instead of a straight line is found, so this is really a "linearization" approach, a fact that Do & Mayfield acknowledge when they looked for an optimal value of n_0. The linearization approach is used frequently in adsorption studies, for example, when a linear adsorption isotherm is used instead of a non–linear one (Weber & Chakravorty, 1974; Rice, 1982; Raghavan & Ruthven, 1983; Mees et al, 1989; Lai & Tan, 1991).

The approach described in this work, i.e. graphical visualization combined with numerical optimization, can be applied to more complex models; for example, models with non-linear isotherms, multicomponent adsorption and branched pore structure. Some of the possibilities will be commented at the Conclusions.

V. CONCLUSIONS AND RECOMMENDATIONS

Five approximate models were developed for the mean intraparticle concentration during adsorption and/or diffusion with negligible external resistance ($Bi \rightarrow \infty$); all of them are more accurate that the reference model of Do & Mayfield (1987). Their simplicity makes them applicable for the design of batch and fixed-bed adsorbers. Three of the models (#1, #2, #2B) are based on a n-order profile for the intraparticle concentration, Equation (2), with a time-dependent exponent n.

While Model #1, represented by Equation (13), is the simplest model replacing the reference one, the most accurate model is Model #3, represented by Equation (20). Models #2 and #2B, represented by Equations (16) and (26), fall between Models #1 and 3 and they are applicable if a relative accuracy of about +2% is accepted. A general expression for n* was found that includes Models #1, 2 and #2B, it can be used to generate more models.

Any of the five models developed in this work represent an improvement with respect to the reference model of Do & Mayfield. The selection of a particular model will depend of the required accuracy: if a simple model is required, then Model #1 can be used; if a more accurate model is required, then Model #3 is recommended. Models #2 and 2B can be used if a relative error of around 2% is acceptable. Model #4 is not recommended as there is not any advantage in using it, when compared with Model #3. Notice that the error limit is associated to very small numbers at the initial adsorption times: $\overline{A}$ has a value of 0.0336 for x = 0.0001 and a 2% error would be equal of 0.0007. The following recommendations are made to continue this research:

1) To develop expressions for the mean intraparticle concentration $\overline{A}$ when the mass transfer resistance at the boundary cannot be neglected, i. e. when the Biot number is finite.
2) To apply these models to the design of batch and fixed-bed adsorbers, which have already been done for the parabolic profile (Liaw, 1979; Rice, 1982; Do & Rice, 1986).

The validity and usefulness of the LDF model and the models developed here are well established; however, there are applications where the underlying assumptions for these models are not valid; for example, when the adsorbent is activated carbon (non-linear isotherm, branched pore structure). Some of these assumptions are:

a) linear adsorption isotherm vs. non-linear isotherm (Langmuir, Freundlich, others);
b) linear driving force vs. quadratic driving force;
c) first order kinetics vs. second order kinetics (Thomas or Hiester-Vermeulen models);
d) one-component adsorption vs. multicomponent adsorption;
e) one type of pore vs. several types of pores (branched, two or more diameters, etc.).

Including the more complex assumptions would add flexibility and applicability to the models developed here, a situation which represents an opportunity of improvement.

VI.   NOTATION

A	constant in Equations (17), (19) and (21)
A	non-dimensional intraparticle solute concentration
$\overline{A}$	mean intraparticle adsorbate concentration; fractional uptake
Bi	Biot number
B	constant in Equations (17), (19) and (21)
C	concentration of adsorbate in fluid phase, kg/m3
C	constant in Table 2
C	constant in Equations (17), (19) and (21)
C'	constant in Table 2
C_0	initial concentration of adsorbate in fluid phase, kg/m3
D	constant in Equations (17)
D_e	effective difussivity, kg/m²s
D_s	surface difussivity, kg/m²s
E	constant in Equations (17), (19) and (21)
$F(x)$	function in Equation (6)
$G(\tau)$	function defined in Table 2
K	adsorption equilibrium constant
K	constant in Equations (23) and (24)
$P(\sqrt{\tau})$	polynomial function related to $G(\tau)$
R	particle radius, m
R	ratio of calculated value versus exact value in Table 3
a	coefficient in Equation (6)
a	constant in Equations (23) and (24)
a_0	coefficient in Equation (2)
a_1	coefficient in Equation (2)
b	coefficient in Equation (6)
b	constant in Equations (23) and (24)
$f(\tau)$	function in Equations (23) and (24)
k	integer number in Equation (4)
k	exponent in Equations (17), (19) and (21)
k_m	external mass transfer coefficient, kg/m²s
n	exponent in Equation (2)
n^*	auxiliary variable defined in Equation (10)
n_0	constant in Equation (27)
q	concentration of adsorbate in particle, kg/m³
$\overline{q}$	mean concentration of adsorbate in particle, kg/m³
t	time, s
x	non-dimensional length inside particle
ρ_P	particle density, kg/m³
τ	non-dimensional time

VII.   REFERENCES

Bhaskar, G. V.; Do, D. D. (1989). A Simple Solution for Nonisothermal Adsorption in a Single Particle. *Chem. Eng. Sci.*, 44 (5), 1215-1219.

Do, D. D.; Rice, R. G. (1986). Validity of the Parabolic Profile Assumption in Adsorption Studies. *AIChE J.*, 32 (1), 149-154.

Do, D. D. and Mayfield, P. L. J. (1987). A New Simplified Model for Adsorption in a Single Particle. *AIChE J.*, 33 (8), 1397-1400.

Do, D. D.; Rice, R. G. (1990). Applicability of the external-diffusion model in adsorption studies. *Chem. Eng. Sci.*, 45 (5), 1419-1421.

Garg, D. R.; Ruthven, D. M. (1975). Linear Driving Force Approximations for Diffusion Controlled

Adsorption in Molecular Sieve Columns. *AIChE J.*, 21 (1), 200-202.

Glueckauf, E. (1955). Theory of Chromatography, Part 10 - Formulae for Diffusion Into Spheres and Their Application to Chromatography. *Trans. Farad. Soc.*, 51, 1540-1551.

Kim, D. H. (1989). Linear Driving Force Formulas for Diffusion and Reaction in Porous Catalysts. *AIChE J.*, 35 (2), 343-346.

Kim, D. H. (2009). Linear Driving Force Formulas for Unsteady-State Diffusion and Reaction in Slab, Cylinder and Sphere Catalyst. *AIChE J.*, 55 (3), 834-839

Lai, C. C. and Tan, C. S. (1991). Approximate Models for Nonlinear Adsorption in a Packed - Bed Adsorber. *AIChE J.*, 37 (3), 461-465.

Li, Z. and Yang, R. T. (1999). Concentration Profile for Linear Driving Force Model for Diffusion in a Particle. *AIChE J.*, 45 (1), 196-200.

Liaw, C.H.; Wang, J.S.P.; Greenkorn, R.A. and Chao, K.C. (1979). Kinetics of Fixed Bed Adsorption: A New Solution. *AIChE J.*, 25 (2), 376–381.

Mees, P. A. J.; Gerritsen, A. W.; Verbeijen, P. J. T. (1989). Fast Calculation of Breakthorugh Curves in Non-Isothermal Fixed-Bed Adsorbers. *AIChE J.*, 35 (8), 1380-1384.

Raghavan, N. S. and Ruthven, D. M. (1983). Numerical Simulation of a Fixed-Bed Adsorption Column by the Method of Orthogonal Collocation. *AIChE J.*, 29 (6), 922-925.

Rice, R. G. (1982). Approximate Solutions for Batch, Packed Tube and Radial Flow Adsorbers – Comparison with Experiment. *Chem. Eng. Sci.*, 37 (1), 83-91.

Sircar, S.; Hufton, J. R. (2000). Why Does the Linear Driving Force Model for Adsorption Kinetics Work? *Adsorption*, 6 (2), 137-147.

Sircar, S.; Hufton, J. R. (2000a). Intraparticle Adsorbate Concentration Profile for Linear Driving Force Model. *AIChE J.*, 46 (3), 659-660.

Subramanian, V. R.; Ritter, J. A.; White, R. E. (2001). Approximate Solutions for Galvanostatic Discharge of Spherical Particles: I. Constant Diffusion Coefficient. *J. of the Electrochem. Soc.*, 148 (11), E444-E449.

Weber, T. W. and Chakravorty, R. K. (1974). Pore and Solid Diffusion Models for Fixed-Bed Adsorbers. *AIChE J.*, 20 (2), 228-237.